New Baryon States in Exclusive Meson Photo-/Electroproduction with CLAS

Victor I. Mokeev and Daniel S. Carman
12000 Jefferson Ave., Newport News, VA 23606, Jefferson Laboratory
(for the CLAS Collaboration)

Received day month year; accepted day month year

Impressive progress achieved in the past decade in experimental studies of exclusive meson photoproduction off protons and global multi-channel amplitude analyses has resulted in the discovery of several long-awaited new nucleon resonances, with a decisive impact from the results of $K\Lambda$ and $K\Sigma$ photoproduction measured with the CLAS detector at Jefferson Lab. Further extension of these efforts towards combined studies of exclusive meson photo- and electroproduction data off protons will be presented. A new excited state of the nucleon, the $N'(1720)3/2^+$, discovered from combined analyses of $\pi^+\pi^- p$ photo- and electroproduction data, in addition to new resonances discovered in photo- and hadroproduction data, demonstrate the promising prospects of this new research avenue for discovery of additional new resonances.

Keywords: New baryon states, Exclusive meson photo- and electroproduction, Charged double pion photo- and electroproduction

PACS: ***75.25.-j, 13.60.-r, 13.88.+e, 24.85.+p***

1. Introduction

Studies of the spectrum of excited nucleon states (N^*) shed light on approximate symmetries of the strong interaction in the regime of large (comparable with unity) QCD running coupling, the so-called strong QCD regime, which underlies the generation of the N^* spectrum [1–5].The full N^* spectrum of nature, including those states already observed and those that are still to be discovered, defines the rate for the transition from the primordial deconfined mixture of quarks and gluons into the hadron gas phase that took place within the first microseconds after the Big Bang [6–8]. In this phase transition the dominant part of hadron mass was generated, chiral symmetry of QCD was broken dynamically, and quark-gluon confinement emerged. These features define the essence of the strong QCD regime that makes the studies of the N^* spectrum a compelling experimental program to explore the emergence of hadron matter from QCD. The recent advances in the search for new excited states of the nucleon, also known as the "missing" resonances, will be presented in this proceedings.

2. "Missing" Resonances from Exclusive Meson Photoproduction Data

Constituent quark models based on approximate symmetries of the strong interaction that are relevant for the strong QCD regime and established by analyzing the N^* spectrum known before 2012 [3–5, 9, 10], predict many more excited states of the nucleon than have been observed in experiments both with electromagnetic and hadronic probes. The expectation from quark models that employ SU(6)×O(3) (spin-flavor×space-rotational) symmetry is depicted in Fig. 1. The predicted and observed nucleon resonances are shown by the filled boxes. The states that are predicted but still not observed are shown by the open boxes. The search for the many states in the mass range above 1.7 GeV that have eluded detection has become the focus of the extensive studies to address the so-called "missing" resonance problem. Quark model expectations of the N^* spectrum starting from the QCD Lagrangian both within lattice and continuum QCD approaches support the states predicted from SU(6)×O(3) symmetry expectations [11–13]. The studies of exclusive meson photoproduction extend the capabilities to search for these resonances in comparison with the results available from exclusive meson hadroproduction with the biggest contribution from data with pion beams. Exclusive meson production with pion beams is sensitive to the resonances with substantial decay into the $N\pi$ final states, while exclusive photoproduction processes allow us to pin down the resonances with decays into $N\pi$ [14] as well as other final hadron states such as $K\Lambda$, $K\Sigma$, and $N\pi\pi$ [15–18]. According to the quark models [3, 5, 19], the non-$N\pi$ final states can strongly couple to the "missing" resonances. The search for these new states has driven the exploration of the N^* spectrum in experiments with electromagnetic probes for the past two decades [20].

Recently, several long-awaited new nucleon resonances were discovered in global multi-channel analyses of exclusive meson photo- and hadroproduction data [21, 22] with a decisive impact of the CLAS results on $K\Lambda$ and $K\Sigma$ photoproduction [15–17]. Implementation of new nucleon resonances in the mass range from 1.8 GeV to 2.2 GeV is essential to describe the data on the $K\Lambda$ and $K\Sigma$ differential cross sections and induced asymmetries at backward angles from CLAS. After the implementation of the new resonances, a good description of the observables for most exclusive photo- and hadroproduction channels relevant in the resonance region and included into the coupled-channel approaches [21,22] was achieved, providing strong evidence for the existence of these new states. The established N^* spec-

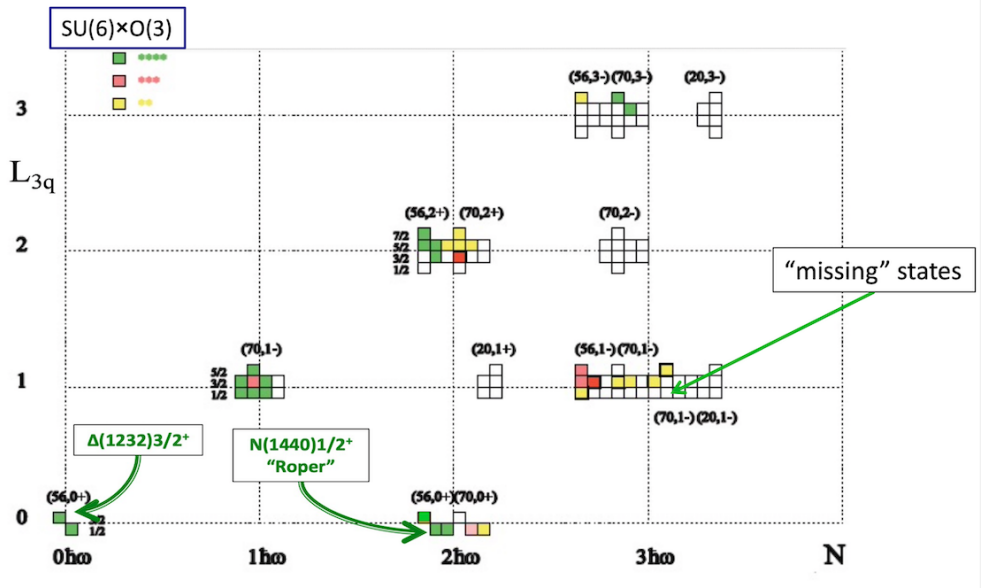

FIGURE 1. Spectrum of nucleon resonances expected in quark models employing $\mathrm{SU}(6)_{\mathrm{spin-flavor}} \times \mathrm{O}(3)_{\mathrm{space}}$ symmetry. L_{3q} is the orbital angular momentum of the three constituent quarks and the quantum number N corresponds to the radial excitation of the three-quark system. The predicted and observed states are shown by the filled boxes, while the predicted and still not observed states are shown by the open boxes.

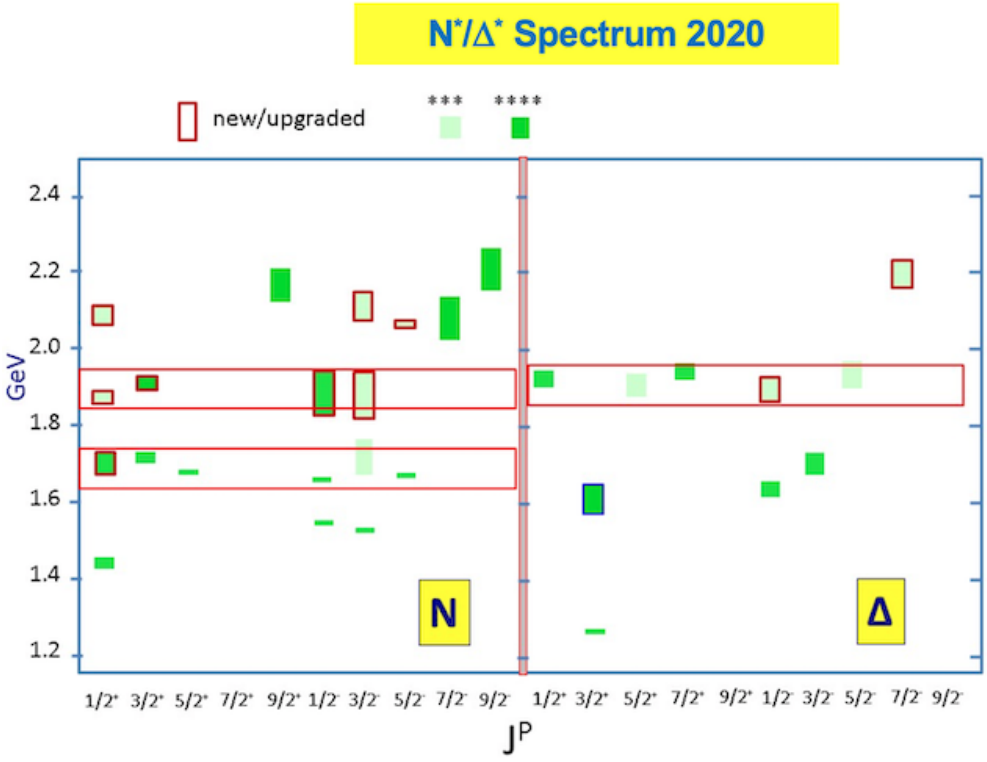

FIGURE 2. The N^* spectrum established in global multi-channel analyses of exclusive meson photo- and hadroproduction data [8]. The recently discovered new resonances are highlighted with the brown boxes.

trum is shown in Fig. 2 with the recently discovered states highlighted with the brown boxes. Two recently discovered resonances, the $N(1895)1/2^-$ and $N(1900)3/2^+$, have been assigned the highest four-star PDG status [23] as firmly established resonances. Knowledge on other recently observed nucleon resonances has been greatly improved as reflected by their current PDG status (increased from two stars to three). The discovery of these new long-awaited resonances repre-

sents an important achievement in hadron physics.

3. The N^* Spectrum from Combined Studies of Exclusive Meson Photo- and Electroproduction Data

Combined studies of exclusive meson photo- and electroproduction data open up new prospects in the exploration of the N^* spectrum. New nucleon resonances seen in photoproduction can be also observed in electroproduction. The resonance masses and the total/partial hadronic decay widths obtained in analyses of exclusive electroproduction data should be the same as established from the exclusive photoproduction data. A successful description of the exclusive meson photo- and electroproduction data within a broad range of photon virtualities Q^2 with Q^2-independent nucleon resonance masses, and total and partial hadronic decay widths, will validate the resonance existence in a nearly model-independent way. The new $N'(1720)3/2^+$ resonance was recently discovered in the combined studies of the CLAS $\pi^+\pi^-p$ photo- and electroproduction data [24] in addition to new resonances established in the analysis of exclusive meson photo- and hadroproduction data [21].

Resonance-like structures were observed a long time ago in the W-dependence of the fully integrated $\pi^+\pi^-p$ electroproduction cross sections from CLAS [25] in the third resonance region (see Fig. 3 with the peak positions at $W \approx 1.71$ GeV in all three Q^2-bins of this measurement). Recently, data on the $\pi^+\pi^-p$ photoproduction cross sections were obtained for W from 1.6-2.0 GeV [18]. In order to explore the resonance contributions into the $\pi^+\pi^-p$ photo- and electroproduction cross sections in the third resonance region, we analyzed nine independent one-fold differential photo-/electroproduction cross sections (see representative examples in Fig. 4). The analysis was carried out within the W-interval from 1.60 GeV to 1.76 GeV for $Q^2 < 1.5$ GeV^2 within the Jefferson Lab/Moscow State University (JM) reaction model [26–28] developed for the extraction of the $\gamma_{r,v}pN^*$ photo-/electrocouplings from combined studies of the $\pi^+\pi^-p$ data. The JM model provides a good description of all data for W up to 2.0 GeV and Q^2 from the photon point up to 5.0 GeV^2. All $\gamma_v pN^*$ electrocouplings obtained from the charged double pion electroproduction channel and included in the PDG have become available from the data analyses within the JM model.

Analysis of the data on the π^+, π^- and p center-of-mass (CM) angular distributions reveals essential contributions from resonances of spin-parity $J^P = 3/2^+$ to $\pi^+\pi^-p$ photo- and electroproduction in the third resonance region. Therefore, we explored two possibilities to describe the $\pi^+\pi^-p$ data in this region: a) either accounting for only conventional resonances with a substantial contribution from the conventional $N(1720)3/2^+$ or b) by implementing on top of the conventional resonances a contribution from a new resonance labeled as $N'(1720)3/2^+$ with mass, $\pi\Delta$ and ρp hadronic decay widths, and photo-/electrocouplings determined from a combined fit of the $\pi^+\pi^-p$ photo- and electroproduction cross sections. In the data fit, we simultaneously varied the parameters of the nucleon resonances and the parameters of the non-resonant mechanisms included in the JM model. Eventually, we selected the computed cross sections with minimal values of χ^2/(data point) in relation to the data. The selected computed cross sections were spread within the data uncertainties for most data points covered by the measurements. Under both assumptions (a) and (b) on the resonant contributions, a good description of the data was achieved. Representative examples are shown in Figs. 3 and 4. The values of χ^2/(data point) obtained from comparison between the measured and computed nine one-fold differential cross sections are comparable for both assumptions.

For the case when the contributions from only conventional resonances are taken into account, the branching fraction for the decay of the conventional $N(1720)3/2^+$ resonance into the ρp final state inferred from the fits of the $\pi^+\pi^-p$ photo- and electroproduction data are different by more than factor of 4 (see Table I). This contradiction conclusively demonstrates that accounting only for the contributions from conventional resonances does not allow us to consistently describe both the $\pi^+\pi^-p$ photo- and electroproduction data. Implementation of the new $N'(1720)3/2^+$ state makes it possible to describe the $\pi^+\pi^-p$ photo- and electroproduction data over the broad range of Q^2 from 0 to 1.5 GeV^2. A good data description was achieved with Q^2-independent masses, with consistent $\pi\Delta$ and ρp hadronic decay widths of the new $N'(1720)3/2^+$ state and of the other conventional resonances with substantial contributions into the $\pi^+\pi^-p$ channel in the third resonance region (see Table II). This provides strong evidence for the existence of the $N'(1720)3/2^+$ resonance.

The masses, total decay widths, and branching fractions for hadronic decays into the $\pi\Delta$ and ρp final states for the conventional $N(1720)3/2^+$ and for the new $N'(1720)3/2^+$ resonances inferred from the data fit are presented in Table III. The $\gamma_{r,v}pN^*$ photo-/electrocouplings of these states derived from fitting the nine independent one-fold $\pi^+\pi^-p$ photo-/electroproduction cross sections are shown in Fig. 5.

We found that for the successful description of the combined $\pi^+\pi^-p$ data, the contributions from both the conventional $N(1720)3/2^+$ and the new $N'(1720)3/2^+$ resonances are needed. These two excited states of the nucleon have almost the same mass, and their total decay widths overlap within the uncertainties for their total hadronic decay widths. However, they have different branching fractions for decays into $\pi\Delta$ and ρp (see Table III). They also have different dependencies of their electrocouplings on Q^2 (see Fig. 5). The differences in their hadronic decays prevent mixing between the $N'(1720)3/2^+$ and $N(1720)3/2^+$ states of the same isospin, spin, and parity. Evidence for two resonances of spin parity $J^P = 3/2^+$ and of isospin 1/2 was obtained in global coupled-channel analyses of exclusive photo-/hadroproduction data [31]. Furthermore, it was found that

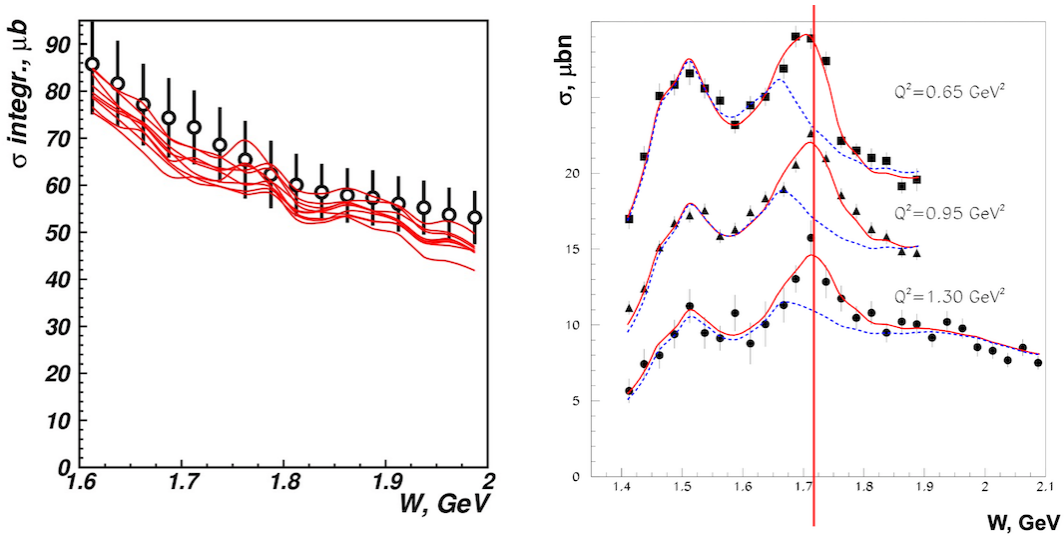

FIGURE 3. Fully integrated $\pi^+\pi^- p$ photo- (left) and electroproduction (right) cross sections as a function of W. The photoproduction data points [18] are shown by the open circles with the statistical and systematic uncertainties added in quadrature. The electroproduction data points are shown by the filled squares with only statistical uncertainties represented. The series of red curves in the left panel represents the computed cross sections within the JM model [26–28] selected in the data fit including the new $N'(1720)3/2^+$. The resonant/non-resonant parameters of the JM model are fit to the data on nine one-fold differential cross sections in each bin of (W, Q^2) covered by the measurements [18, 25]. The description of the fully integrated $\pi^+\pi^- p$ electroproduction cross sections within the JM model accounting for the $N'(1720)3/2^+$ is shown by the red lines in the right panel. The blue dashed curves represents the JM model results from the 2003 version [29,30] accounting for only conventional resonances with the $N(1720)3/2^+$ partial decay width into ρp from the 2002 PDG listings.

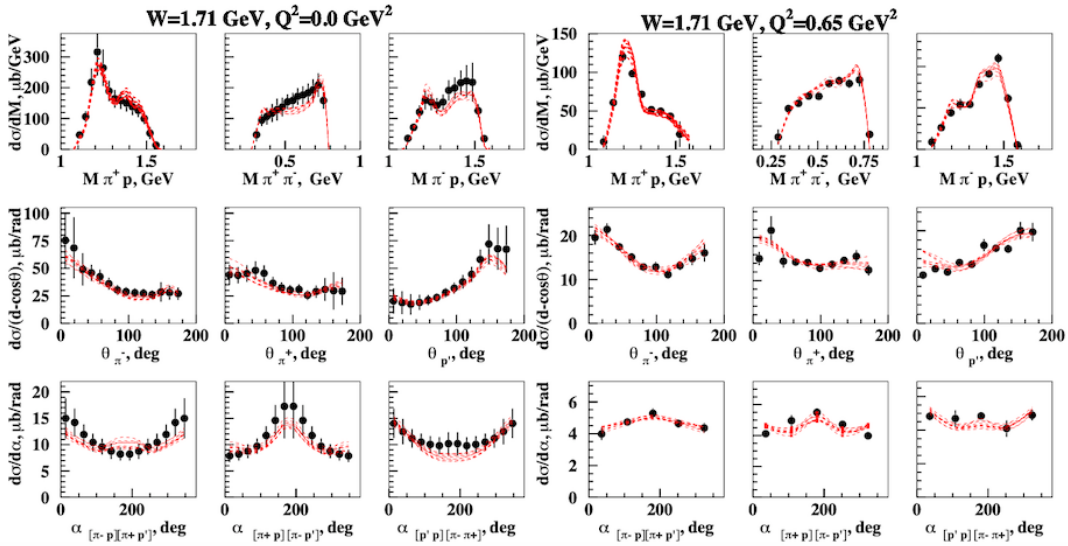

FIGURE 4. Representative examples of the description of the $\pi^+\pi^- p$ one-fold differential cross sections achieved within the JM model [26–28] after implementation of the new $N'(1720)3/2^+$. The computed cross sections selected in the data fit are shown by the red curves.

$N(1720)3/2^+$	N^* total width MeV	Branching fraction for decays to $\pi\Delta$	Branching fraction for decays to ρN
electroproduction	126.0 ± 14.0	64% - 100%	<5%
photoproduction	160.0 ± 65.0	14% - 60%	19% - 69%

TABLE I. $N(1720)3/2^+$ hadronic decay widths and branching fractions into $\pi\Delta$ and ρp determined from independent fits to the data on charged double-pion photo- [18] and electroproduction [25] off protons accounting only for contributions from previously known resonances.

the resonance-like structures observed in the W-dependence of the inclusive electron scattering cross section in the third

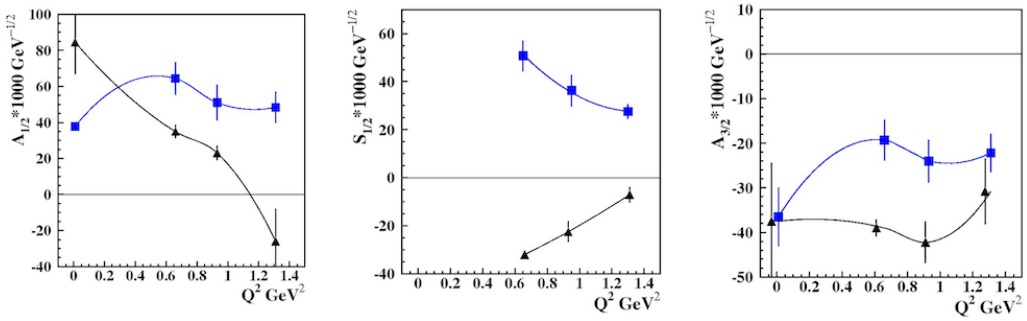

FIGURE 5. The $\gamma_{r,v}pN^*$ photo-/electrocouplings of the conventional $N(1720)3/2^+$ (black) and the new $N'(1720)3/2^+$ (blue) resonances from the $\pi^+\pi^-p$ photo- [18] and electroproduction [25] data fits.

Resonance states	N^* total width MeV	Branching fraction for decays to $\pi\Delta$	Branching fraction for decays to ρp
$\Delta(1700)3/2^-$			
electroproduction	288.0 ± 14.0	77 - 95%	3 - 5%
photoproduction	298.0 ± 12.0	78 - 93%	3 - 6%
N(1720)3/2$^+$			
electroproduction	116.0 ± 7.0	39 - 55%	23 - 49%
photoproduction	112.0 ± 8.0	38 - 53%	31 - 46%
N$'$(1720)3/2$^+$			
electroproduction	119.0 ± 6.0	47 - 64%	3 - 10%
photoproduction	120.0 ± 6.0	46 - 62%	4 - 13%

TABLE II. Hadronic decays into the $\pi\Delta$ and ρp final states of the resonances in the third resonance region with major decays to the $\pi^+\pi^-p$ final state determined from the fits to the data on charged double-pion photo- [18] and electroproduction [25] after implementing a new $N'(1720)3/2^+$ baryon state.

Resonance states	Mass, GeV	N^* total width, MeV	Branching fraction for decays to $\pi\Delta$	Branching fraction for decays to ρp
$N(1720)3/2^+$	1.743-1.753	114 ± 6	38-53%	31-46%
$N'(1720)3/2^+$	1.715-1.735	120 ± 6	47-62%	4-10%

TABLE III. Masses and hadronic decay widths of the $N(1720)3/2^+$ and $N'(1720)3/2^+$ resonances to the $\pi\Delta$ and ρp final states determined as the overlap between the parameter ranges from independent fits of the $\pi^+\pi^-p$ photo- and electroproduction data [18, 25].

resonance region are created with the biggest contribution from the new $N'(1720)3/2^+$ state [32], which supports the existence of this new resonance.

Currently the $N'(1720)3/2^+$ is the only new baryon state for which the results on the Q^2 evolution of the $\gamma_v pN^*$ electrocouplings are available, offering insight into the internal structure of previous "missing" resonances and allowing us to shed light on the peculiar features in their structure that have made their observation so elusive. The electrocouplings of both the $N(1720)3/2^+$ and $N'(1720)3/2^+$ computed within Ads/CFT [33] represent a first promising step in this direction. Analysis of the high-lying nucleon resonance spectrum, as we know it in 2020, suggests SU(6) spin-flavor assignments for the conventional $N(1720)3/2^+$ and the new $N'(1720)3/2^+$ resonances as [56,2^+] and [70,2^+], respectively. These assignments imply: a) both resonances consist of three constituent quarks with orbital angular momentum L=2 and of total quark spin S_q=1/2 [24], b) the new $N'(1720)3/2^+$ resonance represents a system of three bound quarks with orbital excitation over both the ρ and λ coordinates for the three-body system that has been observed for the first time. New data on the $N(1720)3/2^+$ and $N'(1720)3/2^+$ electrocouplings at Q^2 up to 5.0 GeV^2 foreseen from CLAS analyzed within different quark models will allow us to pin down peculiar features in the structure of new baryon states.

4. Conclusions and Outlook

Several long-awaited new "missing" nucleon resonances have been discovered from global analyses of exclusive meson photo- and hadroproduction data with a decisive impact from the $K\Lambda$ and $K\Sigma$ photoproduction channels measured with CLAS. A new $N'(1720)3/2^+$ resonance has been ob-

served in the combined studies of $\pi^+\pi^- p$ photo- and electroproduction data, and this state is the only "missing" resonance for which the results on the Q^2-evolution of the $\gamma_v p N^*$ electrocouplings have become available. In the future, the information on the $N'(1720)3/2^+$ electrocouplings from the CLAS data will be extended towards Q^2 up to 5.0 GeV^2. Analyses of the results on the new resonance electrocouplings in collaborative efforts with hadron structure theory will shed light on the particular features of the "missing" resonance structure that have made them so elusive for detection.

5. Acknowledgments

This material is based upon work supported by the U.S. Department of Energy, Office of Science, Office of Nuclear Physics under contract DE-AC05-06OR23177. The U.S. Government retains a non-exclusive, paid-up, irrevocable, world-wide license to publish or reproduce this manuscript for U.S. Government purposes.

1. S.J. Brodsky *et al.*, Int. J. Mod. Phys. E **29** (2020) 2030006.
2. D.S. Carman, K. Joo, and V.I. Mokeev, Few Body Syst. **61** (2020) 29.
3. S. Capstick and W. Roberts, Prog. Part. Nucl. Phys. **45** (2000) S241.
4. S. Capstick and N. Isgur, Phys. Rev. D **34** (1986) 2809.
5. M.M. Giannini and E. Santopinto, Chin. J. Phys. **53** (2015) 020301.
6. A. Bazavov *et al.*, Phys. Rev. Lett. **113** (1986) 072001.
7. A. Bazavov *et al.*, Phys. Lett. B **737** (2014) 210.
8. V.D. Burkert, EPJ Web Conf **241** (2020) 01004.
9. N. Isgur, G. Karl and R. Koniuk, Phys. Rev. D **25** (1982) 2394.
10. E. Klempt and J.M. Richard, Rev. Mod. Phys. **82** (2010) 1095.
11. R.G. Edwards *et al.*, Phys. Rev. D **84** (2011) 074508.
12. C. Chen *et al.*, Phys. Rev. D **100** (2019) 054009.
13. S. Qin *et al.*, Few Body Syst. **60** (2019) 26.
14. R.A. Arndt *et al.*, Phys. Rev. C **74** (2006) 045205 .
15. R.K. Bradford *et al. (CLAS Collaboration)*, Phys. Rev. C **75** (2007) 035205.
16. M.E. McCracken *et al. (CLAS Collaboration)*, Phys. Rev. C **81** (2010) 025201.
17. B. Dey *et al. (CLAS Collaboration)*, Phys. Rev. C **82** (2010) 025202.
18. E. Golovatch *et al. (CLAS Collaboration)*, Phys. Lett. B **788** (2019) 371.
19. R Bijker *et al.*, Phys. Rev. D **94** (2016) 074040.
20. V.D. Burkert and T.-S.H. Lee, Int. J. Mod. Phys. E **13** (2004) 1035.
21. A.V. Anisovich *et al.*, Phys. Rev. Lett. **119**, 062004 (2017).
22. D. Roenchen *et al.*, Eur Phys.J A **50** (2014) 1035.
23. P.A. Zyla *et al.* Prog. Theor. Exp. Phys. (2020) 083C01.
24. V.I. Mokeev *et al.,* , Phys. Lett. B **805** (2020) 135457.
25. M. Ripani *et al. (CLAS Collaboration)*, Phys. Rev. Lett. **91** (2003) 022002.
26. V.I. Mokeev *et al.*, Phys. Rev. C **80** (2009) 045212 .
27. V.I. Mokeev *et al (CLAS Collaboration)*, Phys. Rev. C **86** (2012) 035203.
28. V.I. Mokeev *et al.*, Phys. Rev. C **93** (2016) 025206.
29. V.I. Mokeev *et al.*, Phys. Atom. Nucl. **64** (2001) 1292.
30. M. Ripani *et al.*, Nucl. Phys. A **672** (2000) 220.
31. H. Kamano *et al.*, Phys. Rev. C **88** (2013) 035209.
32. A.N. Hiller Blin *et al.*, Phys. Rev. C **104**, (2021) 025201.
33. V. Lyubovitskij and I. Schmidt, Phys. Rev. D **102** (2020) 094008.

Table captions.

Table 1. $N(1720)3/2^+$ hadronic decay widths and branching fractions into $\pi\Delta$ and ρp determined from independent fits to the data on charged double-pion photo- [18] and electroproduction [25] off protons accounting only for contributions from previously known resonances.

Table 2. Hadronic decays into the $\pi\Delta$ and ρp final states of the resonances in the third resonance region with major decays to the $\pi^+\pi^- p$ final state determined from the fits to the data on charged double-pion photo- [18] and electroproduction [25] after implementing a new $N'(1720)3/2^+$ baryon state.

Table 3. Masses and hadronic decay widths of the $N(1720)3/2^+$ and $N'(1720)3/2^+$ resonances to the $\pi\Delta$ and ρp final states determined as the overlap between the parameter ranges from independent fits of the $\pi^+\pi^- p$ photo- and electroproduction data [18, 25].

Figure captions.

Figure 1. Spectrum of nucleon resonances expected in quark models employing $\mathrm{SU}(6)_{\mathrm{spin-flavor}} \times \mathrm{O}(3)_{\mathrm{space}}$ symmetry. L_{3q} is the orbital angular momentum of the three constituent quarks and the quantum number N corresponds to the radial excitation of the three-quark system. The predicted and observed states are shown by the filled boxes, while the predicted and still not observed states are shown by the open boxes.

Figure 2. The N^* spectrum established in global multichannel analyses of exclusive meson photo- and hadroproduction data [8]. The recently discovered new resonances are

highlighted with the brown boxes.

Figure 3. Fully integrated $\pi^+\pi^- p$ photo- (left) and electroproduction (right) cross sections as a function of W. The photoproduction data points [18] are shown by the open circles with the statistical and systematic uncertainties added in quadrature. The electroproduction data points are shown by the filled squares with only statistical uncertainties represented. The series of red curves in the left panel represents the computed cross sections within the JM model [26–28] selected in the data fit including the new $N'(1720)3/2^+$. The resonant/non-resonant parameters of the JM model are fit to the data on nine one-fold differential cross sections in each bin of (W, Q^2) covered by the measurements [18, 25]. The description of the fully integrated $\pi^+\pi^- p$ electroproduction cross sections within the JM model accounting for the $N'(1720)3/2^+$ is shown by the red lines in the right panel. The blue dashed curves represents the JM model results from the 2003 version [29, 30] accounting for only conventional resonances with the $N(1720)3/2^+$ partial decay width into ρp from the 2002 PDG listings.

Figure 4. Representative examples of the description of the $\pi^+\pi^- p$ one-fold differential cross sections achieved within the JM model [26–28] after implementation of the new $N'(1720)3/2^+$. The computed cross sections selected in the data fit are shown by the red curves.

Figure 5. The $\gamma_{r,v}pN^*$ photo-/electrocouplings of the conventional $N(1720)3/2^+$ (black) and the new $N'(1720)3/2^+$ (blue) resonances from the $\pi^+\pi^- p$ photo- [18] and electroproduction [25] data fits.